Photoperiod-sensitivity genes (*Ppd-1*): Quantifying their effect on the photoperiod response model in wheat

Authors:

Thomas I. Pérez-Gianmarco [1]

t.perezgianmarco@conicet.gov.ar

+54-2477-439075

Alan D. Severini [2]

severini.alan@inta.gob.ar

Fernanda G. González [1, 2]

gonzalez.f@inta.gob.ar

[1] CITNOBA, CONICET-UNNOBA. Monteagudo 2772 (2700) Pergamino, Buenos Aires, Argentina.

[2] EEA Pergamino INTA. Ruta 32, km 4,5 (2700) Pergamino, Buenos Aires, Argentina.

HIGHLIGHT: *Ppd-1* genes modulate response to photoperiod of timing to anthesis in wheat altering only photoperiod sensitivity, in a less than additive manner, and with no effect on threshold photoperiod or intrinsic earliness.

ABSTRACT: Coupling anthesis date to the best environment is critical for wheat (*Triticum aestivum* L.) adaptation and yield potential. Development to anthesis is controlled by temperature and photoperiod. Response to photoperiod is chiefly modulated by *Ppd-1* genes, but their effect on the quantitative response of i) time to anthesis, and ii) pre-anthesis phases to photoperiod remains largely unknown. A photoperiod-sensitive spring cultivar, Paragon, and near-isogenic lines of it carrying different combinations of *Ppd-1a* insensitivity alleles were tested under a wide range of photoperiods, including switches in photoperiod at the onset of stem elongation. Using multimodel inference we found that *Ppd-1a* alleles reduced photoperiod sensitivity from a) emergence to anthesis and b) emergence to onset of stem elongation, both in a less than additive manner, while threshold photoperiod and intrinsic earliness were unaffected. Sensitivity to current photoperiod from onset of stem elongation to flag leaf and from then to anthesis was milder than for previous phases and was not related to variability in *Ppd-1*. But 'memory' effects of previously experienced photoperiod on the duration from onset of stem elongation to flag leaf, was. The characterisation and quantification provided here of *Ppd-1* allelic combinations' effects on development should help increase genotype-to-phenotype models' accuracy for predicting wheat phenology.

KEYWRODS: Adaptation, development, photoperiod-sensitivity, *Ppd-1*, response to photoperiod, *Triticum aestivum* L. (wheat).

ABBREVIATIONS: AN, anthesis; EM, emergence; FL, flag leaf appearance; NIL, near isogenic line; OSE, onset of stem elongation; *Ppd-1*, *Photoperiod-1* genes; TS, terminal spikelet.

1 Introduction

Coupling anthesis date to the best available environment (i.e. that with the highest photo-thermal coefficient and without frost, heat or water stress) is critical for adaptation and for setting the potential yield of wheat (Fischer, 1975, 1985). Development to anthesis is a continuous process, but it can be divided into phases, according to the structures differentiated by the apex (Slafer and Rawson, 1994) or otherwise. After the imbibition of the seed, leaf primordia are generated in the apex, at *c.* double the rate at which they appear after emergence (EM) (Hay and Kirby, 1991). At some point after a variable number of leaf primordia have been differentiated, the apex starts to elongate and double ridges appear. This indicates that floral initiation has taken place and the apex is now reproductive. However, the final leaf number is not yet defined: uncommitted primordia at the base of the apex can be either committed to be leaves or spikelets. Depending on environmental conditions and genotype, this can happen as late as terminal spikelet differentiation (TS) (Brooking *et al.*, 1995). The onset of stem elongation (OSE), closely associated to TS (Borràs-Gelonch *et al.*, 2011), brings the apex upwards, while leaves continue to appear until the flag leaf is fully expanded (FL, flag leaf ligule visible, DC 39 (Zadoks *et al.*, 1974)). From then onward, the peduncle elongates to carry the spike to its final position, shortly before anthesis in the spike is half-way (AN, DC 65 (Zadoks *et al.*, 1974)). These phenological events can be used to define three distinct pre-anthesis phases: (i) from EM to OSE, when leaves (and spikelets) are differentiated and the final number of leaves is settled, (ii) from OSE to FL, when the stem and spike grow, and leaves appear until the flag leaf is fully expanded, and (iii) from FL to AN, a phase during which the peduncle elongates, and towards the end of which spike dry weight and the number of fertile florets are chiefly determined. This partition in pre-anthesis phases would allow modelling wheat development to anthesis based mostly on leaf differentiation and appearance (Jamieson *et al.*, 2007) and at the same time, enable us to retain information on the duration of particular phases, of agronomic and physiological interest (Slafer and Rawson, 1994), particularly after OSE, when spike weight and grain number are determined.

Wheat development to anthesis is controlled by temperature and photoperiod (Slafer and Rawson, 1994). Temperature can be accounted for either its *per se* effects or through vernalisation, i.e. the hastening of development associated with an exposure of variable length to low temperatures during early development (Davidson *et al.*, 1985;

Griffiths *et al.*, 1985). As wheat is a long-day plant (Vince Prue, 1975), exposure to increasingly long photoperiod hastens its development to anthesis, at a rate named "photoperiod sensitivity" (-days or -ºC days hour^{-1}), until a threshold photoperiod is reached, beyond which the response to photoperiod is saturated and phase duration reaches a minimum (Major, 1980). Such minimum duration of a phase attained once vernalisation and photoperiod requirements have been completely fulfilled is called "intrinsic earliness". Variation in intrinsic earliness among genotypes has been associated to different sensitivity to temperature (Slafer, 1996). These physiological pathways are in turn governed by a series of genes sometimes referred to as "flowering time genes" (Worland, 1996; Snape *et al.*, 2001) or "genetic systems" (Stelmakh, 1997; Kamran *et al.*, 2014): *Vrn*, *Ppd*, and *Eps*. These pathways are integrated downstream to elicit the development of the apex from a vegetative to a reproductive state (Distelfeld *et al.*, 2009; Chen *et al.*, 2014).

Response to photoperiod is largely controlled by the *Ppd-1* major genes, a homeoallelic series of *loci* in the short arms of 2A, 2B, and 2D chromosomes (Scarth and Law, 1984): *Ppd-A1*, *Ppd-B1*, and *Ppd-D1*, respectively (McIntosh *et al.*, 2003). Wild type alleles (*Ppd-1b*) are associated with delayed flowering under short photoperiod, while hastened development (usually called "photoperiod-insensitivity") is associated with either polymorphisms (*Ppd-D1a* or *Ppd-A1a*) (Beales *et al.*, 2007; Wilhelm *et al.*, 2009) or copy number variations (*Ppd-B1a*) (Díaz *et al.*, 2012). Their effect on time to anthesis has been extensively characterised (Scarth *et al.*, 1985; Gonzalez *et al.*, 2005; Bentley *et al.*, 2013; Royo *et al.*, 2015), and reports generally agree that magnitude of the effect each particular allele exerts (i.e. "strength"), follows the ranking *Ppd-D1a* > *Ppd-A1a* > *Ppd-B1a* (Díaz *et al.*, 2012; Shaw *et al.*, 2012; Bentley *et al.*, 2013; Pérez-Gianmarco *et al.*, 2018). Furthermore, a handful of experiments assayed the effect of these genes on the duration of pre-anthesis phases, which *Ppd-1a* alleles shortened with variable strength, generally following the same ranking as for time to anthesis (Whitechurch and Slafer, 2002; Gonzalez *et al.*, 2005; Ochagavía *et al.*, 2017; Pérez-Gianmarco *et al.*, 2018). Pérez-Gianmarco *et al.* (2018) showed that *Ppd-1a* alleles were associated with decreased variability in the duration of the whole cycle to anthesis and of pre-anthesis phases in response to contrasting photoperiod treatments. Nevertheless, only one of them made an attempt to unravel *Ppd-1* genes impact on phase duration and the quantitative response of phase duration to photoperiod by using three chromosome substitution lines, which yielded inconclusive results (Whitechurch and Slafer, 2002).

As all previous studies tested *Ppd-1* allelic combinations under few photoperiod treatments, often limited to just short photoperiod or two extreme, short and long, photoperiods, their effect on the response curve to photoperiod of time to anthesis (i.e. the parameters that define it: photoperiod sensitivity, threshold photoperiod, and intrinsic earliness) remains largely unknown.

Even less information is available about how *Ppd-1* genes affect the response to photoperiod of particular pre-anthesis phases. As durations of pre-anthesis phases within each cultivar could be partially independent from each other (Halloran and Pennell, 1982), it has been proposed that their particular sensitivity to photoperiod might also be independent and, thus, modified as convenient to maximise the spike growth period (Slafer and Rawson, 1996; Slafer *et al.*, 2001). However, for AN to happen a number of already differentiated leaves have to appear first (Jamieson *et al.*, 1998), setting a minimum duration for the subsequent phase, until flag leaf is expanded. The current phase (OSE-FL) is therefore at least somewhat dependent on duration of previous phases (i.e. "memory effect") (Miralles and Richards, 2000). In this paper, we do not only assess the impact of *Ppd-1* genes and their combination on time to anthesis and pre-anthesis phases' response to photoperiod, but also take into account this memory effect from one phase to another.

A number of attempts have been made to adapt agronomic simulation models to predict phenology from genotypic data (White *et al.*, 2008; Zheng *et al.*, 2013), in order to avoid sowing each genotype at different locations and sowing dates to characterise phenology. Although the value of this enterprise has been recognised (Fischer, 2011; He *et al.*, 2012; Yin *et al.*, 2018), prediction of the phenology has been rather poor (White *et al.*, 2008) if compared to the performance of the model calibrated through phenological trials. Better results were obtained by mixing both traditional and genetic approaches, but only a limited number of alleles were assessed (*Ppd-D1a* vs. *Ppd-D1b* in Eagles *et al.*, 2010 and Zheng *et al.*, 2013), limiting the combinations to which inference can be extended. Understanding how *Ppd-1* allelic variants affect the response of timing of anthesis to photoperiod has been pointed out as a solution to the lack of accuracy (He *et al.*, 2012; Bloomfield *et al.*, 2018). The possibility of modelling the duration of pre-anthesis phases, given their different relative importance in determining yield, has also been valued (Fischer, 2011; Zheng *et al.*, 2013). Characterising and quantifying the effects different *Ppd-1* allelic combinations have on the physiological

model of phase duration response to photoperiod would allow for greater accuracy of genotype-to-phenotype simulation models in predicting wheat phenology.

This study aimed to better understand and quantify the effect that *Ppd-1* genes have on the response to photoperiod of time to anthesis and duration of pre-anthesis phases. For this, we studied the rate of response to photoperiod (i.e. photoperiod sensitivity), the intrinsic earliness, and the photoperiod threshold as affected by different combinations of *Ppd-1* genes. Furthermore, we proposed a physiological model considering the response to photoperiod of the three subsequent pre-anthesis phases, taking into account possible memory effects, i.e. the effect the previously experienced photoperiod may have on duration of the following phase.

2 Materials and methods

2.1 Plant material and experiments

Near-isogenic lines (NILs) were developed on cv. Paragon, a triple sensitive (*Ppd-1b*) spring wheat cultivar. Each NIL had one, two or three different *Ppd-1a* alleles, with no more than one *Ppd-1a* allele per genome (Table 1). For *Ppd-B1a*, alleles with copy number variation (Díaz *et al.*, 2012) were used. Detailed methodology of how the NILs were developed can be found in Bentley *et al.* (2013).

Near-isogenic lines were grown in pots during 2012, 2013, 2014, 2017 and 2018 seasons at Pergamino, Argentina (33º 53’ S, 60º 34’ W), with sowing date always within sound agronomic boundaries, from May 29th to July 19th. In order to expose different *Ppd-1* allelic combinations to a range of photoperiods, during 2012 and 2013, they were exposed to either the natural photoperiod of the season or its extension by 6 hours, while for 2014, 2017 and 2018 extension treatments of 2 and 4 hours were added (Figures 1 and 2). During 2018, a late sowing (September 26th) and 6 and 8 hours of photoperiod extension provided exceptionally long photoperiods. All photoperiod values were considered including civil twilight (Figure 1).

Treatments consisted on either a) natural photoperiod exposure from EM to AN, b) natural photoperiod artificially extended from EM to AN, c) transferences from longer to shorter photoperiod at the OSE, or d) transferences from shorter to longer photoperiod at the OSE (see Figures 1 and 2 for variation in environmental variables through the growing seasons and details on treatments, respectively). The photoperiod

extensions were achieved by placing experimental units at a given stage under low-radiation lamps, lit at the sunset (sun below the horizon) and turned off at either 2, 4, 6, or 8 hours after the civil twilight, as described by González *et al.* (2002). Treatments are named throughout the text in the format "hours of photoperiod extension from EM to OSE" / "hours of photoperiod extension from OSE to AN", e.g. "0/0" for continuous natural photoperiod, "0/6" for natural photoperiod until OSE, then six hours of extension over the natural photoperiod from OSE to AN, or "6/6" for continuous extended photoperiod, 6 hours over the natural photoperiod, from EM to AN, etc.

The experimental unit consisted on five plants grown in 7-litre round pots filled with soil. As an exception, during seasons 2014, 2017, and 2018 treatments 0/0, 0/6, and 6/6 were carried out in rectangular-shaped pots (dimensions 0.6 × 0.15 × 0.2 m), each containing ~ 40 plants. Three experimental units (pots) per treatment were grown each season, with exception of 6/6 and 8/8 treatments carried out during the late spring of 2018 and for which two pots were used. During seasons 2012, 2013 and 2014, pots were kept at field conditions, whereas during 2017 and 2018 they were kept in a greenhouse for the whole growth period. Pots were well watered to avoid water stress, and pests and diseases were dealt with accordingly.

Observation of key external phenological stages was performed twice to thrice a week (depending on air temperature), including EM, OSE, FL, and AN, or, as named by Zadoks *et al.* (1974), 10, 31, 39, and 65, respectively. Phenology was assessed at main stems of every experimental unit, and the phenological stage was recorded as having been achieved when at least 50% of the main stems had reached it. Final leaf number was recorded for two plants per pot and the average number was kept as the value for that experimental unit. We used this value and the thermal time elapsed (using 0 ºC as base temperature) between observations to calculate phyllochron (leaf appearance rate $^{-1}$) by relating those using linear regressions. Phase duration was calculated as the thermal time accumulated between any two phenological stages (e.g. Jamieson *et al.*, 1998).

Daily mean temperature was used to calculate accumulated thermal time from emergence at each date, assuming base temperature to be 0ºC. Air temperature was registered by two independent sensors placed under the 0- and 6-hour photoperiod extension treatments at the apex level (when above the ground). The average of both sensors was used as daily mean as they showed no heating effect from the lamps used to

extend the photoperiod. Average photoperiod during a particular phase was calculated by averaging through photoperiod values of each of the days that it lasted for, and thus considers photoperiod variation induced by extension treatments, whether imposed for the whole phase being considered or just part of it (as in the case of treatments involving transferences between photoperiods from EM to AN).

2.2 Modelling photoperiod response as affected by *Ppd-1* genes

In order to characterise and quantify *Ppd-1* genes' effects on the parameters of the response to photoperiod of a) time to anthesis, and b) pre-anthesis phases' duration, we took a multi-model inference approach (Rosen, 2016; Garibaldi *et al.* 2017): For each a) and b), a set of Bayesian hierarchical models were fitted to phase duration (as the dependent variable) and mean photoperiod during that phase or previous phases (as the independent variable). Each model in either set represented a hypothesis of photoperiod response and *Ppd-1* genes' effects on the parameters of such response. Then, the best model of each set was selected based on their parsimony and predictive ability, in contrast to selecting or dropping one variable at a time according with a comparison between their *p*-value and a threshold.

We fitted Bayesian rather than frequentist models because they allowed greater flexibility when specifying the type of response to photoperiod, the effect of *Ppd-1* genes over parameters of that response, and the correlation among those effects (Gelman *et al.*, 2013; Bürkner, 2017). They also allowed us to include prior knowledge on the plausible distribution of the parameters (Wallach *et al.*, 2014): Mildly informative prior distributions were used to protect against over-fitting. Their mean and distribution were set according to prior knowledge of the parameters (Major, 1980; Slafer and Rawson, 1996), visual assessment of raw data and descriptive statistics. Models were fitted using Stan (Carpenter *et al.*, 2017), accessed through the '*brms'* package (Bürkner, 2017) for R (R Core Team, 2018).

Parameters of phase duration response to photoperiod could be unique for all genotypes (population level) or genotype-specific (group level), varying according to the allelic combinations at *Ppd-1* genes: Using hierarchical models allowed us to discern whether a given parameter should best be modelled in a population- or group-level basis, i.e. whether a certain parameter was affected by *Ppd-1* genes or it was accurately described by the same value for the whole population of NILs.

The first set of models was used to describe accumulated thermal time (T_{base} = 0 ºC) from EM to AN as a function of mean photoperiod experienced during that phase. Ten models were proposed in order to test:

a) Whether the response was best described by a linear or bi-linear fit (linear to a threshold photoperiod, then no further response, as proposed by Major (1980)), and
b) which of the parameters that described such response were affected by *Ppd-1* genes:
    i. the rate of change in duration with changes in photoperiod, defined as photoperiod sensitivity (β),
    ii. the constant in the model (α, equal to intrinsic earliness in bi-linear models),
    iii. the threshold photoperiod (point of change in slope, only in bi-linear models, γ), or
    iv. their possible combinations (see details on differences among proposed models in Table 2).

Figure 3 illustrates how the effect of *Ppd-1* genes on the bi-linear model of photoperiod response would hypothetically look like, if they were to affect *only* a) photoperiod sensitivity as proposed in point i., b) threshold photoperiod as proposed in point iii., and c) intrinsic earliness as proposed in point ii. These hypothesis are proposed in the form of models E, I and H, respectively (see Table 2).

The second set of models was comprised of 19 multivariate models, each relating the duration of pre-anthesis phases (EM-OSE, OSE-FL, and FL-AN) to the mean photoperiod during each phase. The models were multivariate since the three response variables, i.e. the durations of pre-anthesis phases were fitted simultaneously. This made it possible to model the correlation between residues resulting from fitting adjacent pre-anthesis phases. Models varied from each other by the way parameters were affected by *Ppd-1* genes and by the shape of the response during the EM-OSE phase, for which both linear and bi-linear responses were proposed (see Table 3). No models were proposed that considered bi-linear responses during OSE-FL and FL-AN phases as such responses were not evident from raw data. Summarising, variation among the models considered whether

a) a threshold for response to photoperiod of the EM-OSE phase existed,
b) one, two or the three phases responded to photoperiod,
c) response during OSE-FL was conditioned by the photoperiod experienced previously (during EM-OSE),
d) different *Ppd-1* genes affected the parameters describing photoperiodic response on each phase differently, and
e) correlations between the effect of *Ppd-1* genes on parameters of current and following phases were included in the model.

For a full description of each particular model see Table 3.

Once the models were fitted, the best ones from each set were selected by their expected predictive accuracy from comparing 10-fold cross validation results using the 'loo_compare' function from the 'loo' package (Vehtari *et al.*, 2017) in R. Also, within each set of models, we screened the magnitude of prospective *Ppd-1* genes' effects on model parameters relative to the population mean in the most complex models to assess the value of group effects in the model. The multivariate nature of the second set of models forced a larger number of possible combinations often differing in one or few parameters. Under these circumstances, selecting the best model by comparing cross-validation results only, could lead to selecting an over-fitted model (Piironen and Vehtari, 2017), i.e. their parameters not necessarily reflecting the outcome of physiological processes or metabolic pathways. For this reason, the best models according to expected predictive accuracy were tested against the rest of the top-performing models using Bayes factors (K), a measure of how well, relative to each other, the models explained the data, according to Lavine and Schervish (1999). We selected the model with greatest likelihood (if $K > 10^1$ (Kass and Raftery 1995)) and fewest parameters. Together with analysing genes' relative effects, this method allowed to us to avoid selecting over-fitted models. Estimates of R^2 for each phase and root mean square error (RMSE) for anthesis date were provided as a measure of goodness of fit of each model, but they were not used to select models, as they do not necessarily reflect their predictive ability (Wallach *et al.*, 2014; McElreath, 2015).

3 Results

3.1 Time to anthesis

Across all years and photoperiod treatments, a wide range of values of mean photoperiod from emergence to anthesis was explored, from 11.3 to 22.4 h. Accumulated thermal time to anthesis varied from ~ 770 to 2140 ºC d. A fraction, that ranged from 0 to 50 % through seasons, of the experimental units sown with Paragon and exposed to natural photoperiod until OSE (< 12.5 h) did not progress into stem elongation in the main culm and eventually died before the end of the experiment. Dissection of a sample of the plants showing these symptoms showed stalled development of the apex shortly after terminal spikelet had been differentiated. This was considered to be a qualitative response and was therefore not accounted for in the quantitative models proposed.

Model E (Equation 1, Figure 4) was chosen by cross-validation as the most parsimonious and with best predicting ability (Table 4). While some more complex models performed equally well in cross-validation (Table 4), examination of *Ppd-1* genes' effects showed negligible relative effects on model parameters other than photoperiod sensitivity, which is evidence of over-fitting (Supplementary Figure 1). Besides, model E showed no meaningful penalisation of goodness of fit when compared against models with more parameters: it averaged values of R^2 of 71 % and RMSE of 106 ºC d (see Table 4 for a full comparison among models).

Model E is described by equation 1:

$$y_{ij} \sim N(\mu_{ij}, \sigma_y^2)$$

$$\mu_{ij} = \begin{cases} \alpha + \beta_j\,(x_{ij} - \gamma), & \text{if } x_{ij} < \gamma \\ \alpha, & \text{otherwise} \end{cases} \qquad (1)$$

$$\beta_j \sim N(\beta, \sigma_\beta^2)$$

where y_{ij} is the phase duration from EM to AN of observation i of genotype j, x_{ij} is the mean photoperiod from EM to AN from observation i of genotype j, μ_{ij} is the fitted phase duration, σ_y^2 is the error variance, α is the intrinsic earliness, β_j is the photoperiod

sensitivity of genotype j, γ is the photoperiod threshold, β is the population (mean) photoperiod sensitivity, and σ_β^2 is the genotype variance of the photoperiod sensitivity.

This has two implications, both illustrated in Figure 4. First, it confirmed the bi-linear response of thermal time to anthesis to photoperiod. Accumulated thermal time to anthesis decreased as photoperiod increased, at a certain rate (i.e. β_j, photoperiod sensitivity, the slope in Figure 4), until a threshold photoperiod (γ, abscissa for slope change in Figure 4) was reached in which accumulated thermal time to anthesis was minimum, (i.e. α, intrinsic earliness, the constant in Figure 4). Beyond this threshold, there was no response of hastening anthesis to increasing photoperiod.

Second, and most important, it characterised and quantified the effect of *Ppd-1* genes on model parameters. The addition of *Ppd-1a* alleles on a sensitive background (and their stacking on an already insensitive one) decreased photoperiod sensitivity of such resulting genotype (β_j), the only parameter affected by variation in *Ppd-1* genes. Photoperiod sensitivity ranged from ~ -160 ºC d h^{-1} in Paragon to ~ -45 ºC d h^{-1} in the triple *Ppd-1a* NIL "PGS1002A+CS2B+S642D" (Figure 4, Table 5). Threshold photoperiod (γ) and intrinsic earliness (α) remained constant for all genotypes tested, and reached values of ~ 18.3 h (CI 90% 18.0, 18.5) and ~ 850 ºC d (CI 90% 835, 869) respectively (Figure 4).

Introgression of any single *Ppd-1a* allele to the triple sensitive background, i.e. Paragon, caused photoperiod sensitivity to drop (Figures 4 and 5). The magnitude of such reduction depended on the specific allele being introduced: While the mildest alleles (*Ppd-B1a* from Chinese Spring or Recital) almost halved photoperiod sensitivity as compared to that of Paragon, the strongest allele (*Ppd-D1a* from Opata) brought it to be less than a third of it (Table 5). In general, and averaging different allelic variants, the order of strength of the alleles according to the chromosome to which they belong was *Ppd-D1a* > *Ppd-A1a* > *Ppd-B1a* (Table 5). This can be observed in Figure 4, as the difference in the reduction in slopes caused by different *Ppd-1a* alleles being introduced when compared to Paragon, and the marginal effect from their triple stacking in PGS1002A+CS2B+S642D.

Stacking insensitive alleles in numbers greater than one also reduced photoperiod sensitivity (Figure 5, Table 5). But while the magnitude of such effect was also affected by the single- *Ppd-1a* -NIL against which the comparison is drawn, it was never of the

same magnitude as when introgressing the first *Ppd-1a* allele in a triple sensitive background (Figure 5, Table 5). The marginal effect of adding a *Ppd-D1a* allele to an already insensitive, but single- *Ppd-1a* NIL varied from ~ 40ºC d h $^{-1}$ if compared to PCS2B to almost half of it if compared to PGS1002A (Table 5). In fact, double *Ppd-1a* NILS were little, if any, more insensitive than PO2D when they carried a *Ppd-D1a* allele, showing saturation of the response to additional insensitivity alleles on a background with already strong insensitivity (Table 5, Figure 5). In the case of a third insensitivity allele being introgressed, it did not reduce photoperiod sensitivity more than 14 ºC d h $^{-1}$ in any case, and it usually had an even lesser effect (Figure 5). In summary, the effect of stacking and additional *Ppd-1a* allele was never additive, and heavily depended upon the strength of the allele(s) already introgressed (or the insensitivity of the line on which it was introgressed).

3.2 Duration of pre-anthesis phases

All pre-anthesis phases were exposed to photoperiods ranging from 10.9 to 21.9 h, 11.2 to 22.8 h, and 11.9 to23.0 h for EM-OSE, OSE-FL, and FL-AN, respectively. Variation was achieved in the duration of such phases, with minimum durations of ~ 300, 70, and 115 ºC d and maximums of up to ~ 1315, 780, and 545 ºC d, respectively.

Models T, U, and V (Table 4) all performed considerably better than the rest as for their predicting ability. Model T, however, was better supported by the data according to the comparison through Bayes factors (*K*, Table 6), with the added value of using considerably fewer parameters than models U and V (see Table 3 for detail on models' parameters). This did not imply a penalisation in goodness of fit of model T when compared to the more complex models U and V (see Table 6). Further examination of *Ppd-1* genes' effect on parameters of the most complex models (models U and V) showed evidence of overfitting: Genes' effects on parameters additional to those proposed by model T were negligible in either absolute or relative values (Supplementary Figure 2), and the more complex models provided less accurate estimations of those parameters most likely affected by *Ppd-1* genes (Supplementary Figure 2). Model T (Equation 2, Table 3, Figure 6) was then chosen from all the proposed models for having the greatest likelihood, balancing predicting ability and parsimony with goodness of fit (see Table 6 for the full comparison of models).

Model T is described by equation 2:

$$y_{ij}^{\mathrm{EM-OSE}} \sim N(\mu_{ij}^{\mathrm{EM-OSE}}, \sigma_y^{2,\mathrm{EM-OSE}})$$

$$y_{ij}^{\mathrm{OSE-FL}} \sim N(\mu_{ij}^{\mathrm{OSE-FL}}, \sigma_y^{2,\mathrm{OSE-FL}})$$

$$y_{ij}^{\mathrm{FL-AN}} \sim N(\mu_{ij}^{\mathrm{FL-AN}}, \sigma_y^{2,\mathrm{FL-AN}})$$

$$\mu_{ij}^{\mathrm{EM-OSE}} = \begin{cases} \alpha^{\mathrm{EM-OSE}} + \beta_j^{\mathrm{EM-OSE}} (x_{ij}^{\mathrm{EM-OSE}} - \gamma^{\mathrm{EM-OSE}}), & \text{if } x_{ij}^{\mathrm{EM-OSE}} < \gamma^{\mathrm{EM-OSE}} \\ \alpha^{\mathrm{EM-OSE}}, & \text{otherwise} \end{cases}$$

$$\mu_{ij}^{\mathrm{OSE-FL}} = \alpha_j^{\mathrm{OSE-FL}} + \beta^{\mathrm{OSE-FL}} x_{ij}^{\mathrm{OSE-FL}} + \delta_j^{\mathrm{OSE-FL}} x_{ij}^{\mathrm{EM-OSE}} \quad (2)$$

$$\mu_{ij}^{\mathrm{FL-AN}} = \alpha_j^{\mathrm{FL-AN}} + \beta^{\mathrm{FL-AN}} x_{ij}^{\mathrm{FL-AN}}$$

$$\beta_j^{\mathrm{EM-OSE}} \sim N(\beta^{\mathrm{EM-OSE}}, \sigma_\beta^{2,\mathrm{EM-OSE}})$$

$$\alpha_j^{\mathrm{OSE-FL}} \sim N(\alpha^{\mathrm{OSE-FL}}, \sigma_\alpha^{2,\mathrm{OSE-FL}})$$

$$\delta_j^{\mathrm{OSE-FL}} \sim N(\delta^{\mathrm{OSE-FL}}, \sigma_\delta^{2,\mathrm{OSE-FL}})$$

$$\alpha_j^{\mathrm{FL-AN}} \sim N(\alpha^{\mathrm{FL-AN}}, \sigma_\alpha^{2,\mathrm{FL-AN}})$$

where $y_{ij}^{\mathrm{EM-OSE}}$, $y_{ij}^{\mathrm{OSE-FL}}$ and $y_{ij}^{\mathrm{FL-AN}}$ are, respectively, the durations of phase EM-OSE, OSE-FL, and FL-AN from observation i of genotype j; $x_{ij}^{\mathrm{EM-OSE}}$, $x_{ij}^{\mathrm{OSE-FL}}$, and $x_{ij}^{\mathrm{FL-AN}}$ are, respectively, the mean photoperiod of phase EM-OSE, OSE-FL, and FL-AN from observation i of genotype j; $\mu_{ij}^{\mathrm{EM-OSE}}$, $\mu_{ij}^{\mathrm{OSE-FL}}$, and $\mu_{ij}^{\mathrm{FL-AN}}$ are the fitted phase durations of EM-OSE, OSE-FL and FL-AN; $\sigma_y^{2,\mathrm{EM-OSE}}$, $\sigma_y^{2,\mathrm{OSE-FL}}$, and $\sigma_y^{2,\mathrm{FL-AN}}$ are the error variances of each phase; $\alpha^{\mathrm{EM-OSE}}$ is the intrinsic earliness of phase EM-OSE; $\beta_j^{\mathrm{EM-OSE}}$ is the photoperiod sensitivity of genotype j during phase EM-OSE; $\gamma^{\mathrm{EM-OSE}}$ is the photoperiod threshold of phase EM-OSE; $\beta^{\mathrm{EM-OSE}}$ is the mean, and $\sigma_\beta^{2,\mathrm{EM-OSE}}$ is the genotype variance, of the photoperiod sensitivity of phase EM-OSE;

$\alpha_j^{\mathrm{OSE-FL}}$ is the constant of genotype j, $\delta_j^{\mathrm{OSE-FL}}$ is the sensitivity to previous (i.e. EM-OSE) photoperiod of genotype j during phase OSE-FL, $\alpha^{\mathrm{OSE-FL}}$ is the mean, and $\sigma_\alpha^{2,\mathrm{OSE-FL}}$ is the genotype variance, of the constant of phase OSE-FL, $\delta^{\mathrm{OSE-FL}}$ is the mean, and $\sigma_\delta^{2,\mathrm{OSE-FL}}$ is the genotype variance, of the sensitivity of phase OSE-FL to previous photoperiod. $\alpha_j^{\mathrm{FL-AN}}$ is the constant of genotype j, $\alpha^{\mathrm{FL-AN}}$ is the mean, and $\sigma_\alpha^{2,\mathrm{FL-AN}}$ is the genotype variance, of the constant of phase FL-AN. Also modelled were the correlation between parameters $\beta_j^{\mathrm{EM-OSE}}$ and $\alpha_j^{\mathrm{OSE-FL}}$, and the correlation between residuals of each phase.

According to model T, all three pre-anthesis phases were shortened as photoperiod increased (Figure 6), but the shape and magnitude of their quantitative response, and the effect of Ppd-1 genes on such response, were very different. A bi-linear response was found only in the EM-OSE, with a threshold photoperiod 16 ± 0.16 h and an intrinsic earliness that averaged ~ 430 ± 3 ºC d. Photoperiod sensitivity, in turn, varied with genotypes. In general, the addition of any *Ppd-1a* reduced photoperiod sensitivity when compared to the triple sensitive Paragon (~ -140ºC d h $^{-1}$). The magnitude of such reduction depended on the allele introgressed, following the trend described for their effect on photoperiod sensitivity for the whole phase from EM to AN. The addition of *Ppd-B1a* from Chinese Spring on the triple sensitive background, for example, reduced photoperiod sensitivity to ~ -70 ºC d h $^{-1}$, almost halving that of Paragon, while *Ppd-D1a* from Opata dropped it further to ~ -40 ºC d h $^{-1}$ (Table 5). Also, the stacking of two or three *Ppd-1a* alleles further reduced photoperiod sensitivity: the triple-insensitive genotype with *Ppd-1a* alleles in A, B and D genomes from GS-100, Chinese Spring and Sonora 64, respectively, reached levels of sensitivity as low as ~ -30 ºC d h $^{-1}$. Again, the magnitude of this effect depended on the "strength" of the allele already being considered. However, under no circumstances was this effect additive, i.e. it did not reduce the photoperiod sensitivity of the already insensitive genotype to the same extent as when compared to its sole effect on Paragon.

In contrast to EM-OSE phase, both OSE-FL and FL-AN phases showed a linear response to current photoperiod, shortening with increasing photoperiod, with no observed threshold up to 22.8 and 23 h in average, respectively (see contrast between panels in Figure 6). Quantitative response to current photoperiod was unique across

NILs, averaging ~ -11ºC d h^{-1} (CI 90% 10, 12) during OSE-FL (β^{OSE-FL}), while the lowest response was during the FL-AN phase (β^{FL-AN}, ~ -8ºC d h^{-1}, CI 90% 7, 10).

For the OSE-FL phase, *Ppd-1a* alleles reduced its duration through decreasing the constant α_j^{OSE-FL}, that changed its value when x_{ij}^{OSE-FL} was equalled to 0 from ~ 940 (Paragon) to ~ 500 ºC d (triple-insensitive genotypes) (see Table 5), and through reducing the sensitivity of OSE-FL to photoperiod experienced during the previous EM-OSE phase (δ_j^{OSE-FL}). *Ppd-1* genes did not affect the sensitivity to current photoperiod, β^{OSE-FL}, which was shared among genotypes (notice the absence of the *j* sub-index in the photoperiod sensitivity of the parameter, making it independent of the *j*-genotype). The effect *Ppd-1* genes had on parameters α_j^{OSE-FL} and δ_j^{OSE-FL} was highly correlated with their effect on photoperiod sensitivity during the EM-OSE phase β_j^{EM-OSE} (r = -0.87 and r = 0.85, respectively).

The effect *Ppd-1a* alleles had on the FL-AN phase was considerably milder and only limited to the constant of the response, α_j^{FL-AN}, which was decreased by them. This effect was much milder than for the OSE-FL phase, though: when x_{ij}^{FL-AN} was equalled to 0, it averaged ~ 415 ºC d for Paragon and ~ 380 ºC d for the triple-insensitive genotypes, with their posterior distributions overlapping considerably (see Table 5). If described in terms of phyllochrons, the constant averaged 2.40 (CI 90% 2.36, 2.46). This relationship was negligibly affected by average photoperiod during FL-AN (-0.08 phyllochrons h^{-1}, CI 90% -0.07, -0.09).

3.3 *Ppd-1* effects on final leaf number and leaf appearance dynamics

Ppd-1a alleles reduced the number of leaves on the main culm. This effect was most noticeable under shorter photoperiod (+0 and +2 treatments in Table 7), as expected. This was observed both when single *Ppd-1a* NILs were compared against Paragon, and as a result of stacking, when comparing double or triple *Ppd-1a* genotypes against single or double *Ppd-1a* genotypes, respectively. Similar to the impact on phase duration, *Ppd-1a* alleles' effect under short photoperiod varied in magnitude, when they were the only source of insensitivity. *Ppd-D1a*-bearing genotypes produced up to ~ 3 fewer leaves than the triple-sensitive Paragon, while some *Ppd-B1a*-bearing ones reduced Paragon's final leaf number by only ~ 2 (Table 7). The magnitude of single-allele effect grew with the insensitivity provided by the allele for the EM-OSE phase.

Stacking any two *Ppd-1a* alleles yielded approximately the same results in terms of final leaf number with no extension of natural photoperiod (8.2 to 8.7 leaves), and differences with stacking a further third allele were always less than a leaf. As photoperiod grew longer during the EM-OSE phase, the effect of *Ppd-1a* alleles on final leaf number decreased, to the point of no differences being observable under 8 hours of photoperiod extension. Under such condition, both very insensitive and sensitive genotypes had their final leaf number reduced to 6-7 leaves (Table 7).

Final leaf number showed a positive correlation with thermal time accumulated from emergence to FL (i.e. EM-OSE + OSE-FL), without distinguishing among genotypes (0.73, CI 90% 0.70, 0.75). Phyllochron values averaged ~ 108 ºC d h^{-1}. While phyllochron showed a mild response to photoperiod (~ -2.2 ºC d leaf $^{-1}$ per hour of increase in photoperiod), no effect of *Ppd-1* on this trait could be detected (data not shown).

4 Discussion

Ppd-1 genes altered photoperiod sensitivity of the EM-AN phase without affecting either threshold photoperiod or intrinsic earliness (Figure 4). This agrees with the only other known report on *Ppd-1* and photoperiod response, which used three chromosome substitution lines carrying two different *Ppd-1* alleles (Whitechurch and Slafer, 2002). Here, we not only characterised *Ppd-1* effects on response to photoperiod, but we quantified the effect of five different *Ppd-1* alleles, as well as all their double and triple combinations for the first time. In particular, *Ppd-1a* alleles reduced photoperiod sensitivity and the magnitude of the effect depended on which particular allele was considered (Table 5). In this paper we showed how the effect of single *Ppd-1a* alleles on time to anthesis under short photoperiod as reported in previous studies (González *et al.* 2005; Díaz *et al.*, 2012; Shaw *et al.*, 2012; Bentley *et al.*, 2013; Pérez-Gianmarco *et al.*, 2018) is exclusively due to their effect on photoperiod sensitivity, i.e. as they reduce photoperiod sensitivity, the cycle to anthesis is shortened. Furthermore, the quantification of the effect that different *Ppd-1* alleles and their combination have on photoperiod sensitivity (Table 5) is useful for breeding time to anthesis of new cultivars by linking particular *Ppd-1* combinations to the desired photoperiod response. Also, it is

a valuable asset for improving the predictive ability of gene-based simulation models, as recognised by White *et al.* (2008) and Bloomfield *et al.* (2018).

Stacking *Ppd-1a* alleles also reduced photoperiod sensitivity, but the reduction caused by any given allele depended on a) the insensitivity provided by the already-introgressed allele, and b) the strength of the allele being introgressed. In any case, the effect of the second (or third) introgressed allele was never additive, i.e. it never accounted for as much insensitivity as when introgressed on the triple sensitive (or single insensitive) background (Table 5). The saturation response for photoperiod sensitivity to the stacking of *Ppd-1a* alleles observed in this paper (see Figure 5) explains the saturation response in terms of phase duration that has been recognised before by Shaw *et al.* (2012) and Pérez-Gianmarco *et al.* (2018) and is in line with the molecular model of the flowering pathway in which *Ppd-1* participates.

Modelling photoperiod response to anthesis by partitioning the cycle in pre-anthesis phases allowed us to better understand and quantify *Ppd-1* genes' effects on the mechanisms of such response, if compared to the "whole-cycle" approach. Moreover, switching photoperiod treatments at OSE, when the final number of leaves is already set, allowed us to expose plants to independent photoperiods before and after OSE without altering final leaf number. As a result, we were able to model and quantify a "memory" effect during OSE-FL as a variation in duration in response to previously experienced photoperiod (during EM-OSE) as opposed to the variation in duration in response to current photoperiod during OSE-FL. While the former would be conveyed by leaves yet to appear at OSE, the latter would be necessarily determined by variations in phyllochron in response to current photoperiod, since the number of leaves to appear had already been determined. Remarkably, the accuracy of the prediction of time to anthesis was not harmed by predicting the duration of pre-anthesis phases, but rather improved from 106 ºC d (model E) to 101 ºC d (model T) of RMSE (Tables 4 and 6, Figure 7).

Through this approach we found *Ppd-1* genes to affect the response of particular pre-anthesis phases to photoperiod differently (Figure 6). *Ppd-1a* alleles reduced sensitivity to current photoperiod only during the EM-OSE phase, in a magnitude equivalent to that of their effect on photoperiod sensitivity of the whole cycle to anthesis. In contrast, no effect of *Ppd-1a* alleles on sensitivity to current photoperiod during OSE-FL or FL-AN phases could be detected. This is reasonable, at least for the OSE-FL phase, since no

Ppd-1 allelic combinations were detected to show a particular response of phyllochron to current photoperiod. However, *Ppd-1* genes did affect the average duration of OSE-FL and FL-AN phases. While their effect on the duration of the peduncle elongation phase (i.e. FL-AN) was very limited, they had considerable impact on the magnitude of "memory" effects during the OSE-FL phase: The duration of the OSE-FL phase in genotypes with higher photoperiod sensitivity during the EM-OSE phase was found to be higher in average and to respond more steeply, i.e. be more sensitive, to photoperiod experienced previously than that of more insensitive genotypes, as variation in $\alpha_j^{\text{OSE-FL}}$ and $\delta_j^{\text{OSE-FL}}$ shows (Table 5). This can be understood as a result of final leaf number being both higher in average and more variable through photoperiod treatments during EM-OSE in highly sensitive genotypes than in the insensitive ones: Paragon plants being transferred from short (+0) to long (+8) photoperiod at OSE, would still have to appear ~ 3.5 leaves more than triple insensitive NILs, irrespective of current photoperiod during OSE-FL (Table 7).

The effect of single *Ppd-1a* alleles on early development (i.e. until OSE) partially agrees with that reported by Whitechurch and Slafer (2002). However, in contrast with our study, they reported differing photoperiod sensitivity among lines carrying different *Ppd-1* combinations for the TS-AN phase (equivalent to OSE-AN phase as described in this paper). A possible source for this divergence is the fact that their treatments did not include transferences between photoperiod treatments at TS, but kept all photoperiod treatments constant from EM to AN instead. Current photoperiod during the TS-AN phase was then highly correlated to photoperiod experienced previously, and response to current photoperiod, necessarily confounded with memory effects (further discussion can be found in Slafer *et al.* 1994).

In the light of these results, it would seem unlikely that variation at the *Ppd-1* loci could allow modifying the relative duration of particular pre-anthesis phases with aims of increasing yield potential. However, it has been reported that *Ppd-1a* could affect the duration of a specific pre-anthesis phase more than the duration of others (Scarth *et al.*, 1985; Foulkes *et al.*, 2004; Gonzalez *et al.*, 2005; Ochagavía *et al.*, 2017) and there is evidence of variability in the sensitivity of phyllochron to photoperiod in different cultivars (Slafer and Rawson, 1997; Miralles and Richards, 2000; Miralles *et al.*, 2003; Whitechurch *et al.*, 2007), causing pre-anthesis phases to respond to current photoperiod differently among them. While photoperiod sensitivity in this analysis was estimated

taking into account every data point irrespective of which photoperiod they experienced in previous pre-anthesis phases, quantifying the effect of *Ppd-1a* alleles on direct response to photoperiod during later development would need different previous photoperiod treatments to be considered separately, to avoid confusion from memory effects. This analysis, to be presented in a following paper, should be conclusive about the effect *Ppd-1* genes have on the balance between memory and direct effects of photoperiod on phase duration.

This paper presented a novel analysis for a comprehensive characterisation of *Ppd-1* effects on response to photoperiod of time to anthesis and pre-anthesis phases duration. Also, this analysis allowed us to quantify the effects of five different *Ppd-1a* alleles, as well as all their double and triple combinations on photoperiod sensitivity for the first time. This quantification is remarkably useful for tailoring time to anthesis when developing new cultivars and a valuable asset for improving the predictive ability of gene-based simulation models.

5 Awknowledgements

We thank David Laurie and Simon Griffiths from John Innes Centre (UK) for providing the seeds of the NILs used in this study. The experimental work was supported by EU-FP7/ADAPTAWHEAT 289842, PNCyO 1127042 (INTA), SIB 2017 and SIB 2019 (UNNOBA) grants. TI Pérez-Gianmarco held a doctoral fellowship from CONICET (Consejo Nacional de Investigaciones Científicas y Técnicas).

6 References

Beales J, Turner A, Griffiths S, Snape JW, Laurie DA. 2007. A Pseudo-Response Regulator is misexpressed in the photoperiod insensitive Ppd-D1a mutant of wheat (Triticum aestivum L.). Theoretical and Applied Genetics **115**, 721–733.

Bentley AR, Horsnell R, Werner CP *et al.* 2013. Short, natural, and extended photoperiod response in BC2F4 lines of bread wheat with different Photoperiod-1 (Ppd-1) alleles. Journal of Experimental Botany **64**, 1783–1793.

Bloomfield MT, Hunt JR, Trevaskis B, Ramm K, Hyles J. 2018. Ability of alleles of PPD1 and VRN1 genes to predict flowering time in diverse Australian wheat (Triticum aestivum) cultivars in controlled environments. Crop and Pasture Science **69**, 1061–1075.

Borràs-Gelonch G, Rebetzke GJ, Richards RA, Romagosa I. 2011. Genetic control of duration of pre-anthesis phases in wheat (Triticum aestivum L.) and relationships to leaf appearance, tillering, and dry matter accumulation. Journal of Experimental Botany **63**, 69–89.

Brooking IR, Jamieson PD, Porter JR. 1995. The influence of daylength on final leaf number in spring wheat. Field Crops Research **41**, 155–165.

Bürkner P-C. 2017. Brms: An R Package for Bayesian Multilevel Models Using Stan. Journal of Statistical Software **80**, 1–28.

Carpenter B, Gelman A, Hoffman MD, Lee D, Goodrich B, Betancourt M, Brubaker M, Guo J, Li P, Riddell A. 2017. Stan: A Probabilistic Programming Language. Journal of Statistical Software **76**, 1–32.

Chen A, Li C, Hu W, Lau MY, Lin H, Rockwell NC, Martin SS, Jernstedt JA, Lagarias JC, Dubcovsky J. 2014. PHYTOCHROME C plays a major role in the acceleration of wheat flowering under long-day photoperiod. Proceedings of the National Academy of Sciences **111**, 10037–10044.

Davidson JL, R CK, Jones DB, Bremner PM. 1985. Responses of Wheat to Vernalization and Photoperiod. Australian Journal of Agricultural Research **36**, 347–359.

Distelfeld A, Li C, Dubcovsky J. 2009. Regulation of flowering in temperate cereals. Current Opinion in Plant Biology **12**, 178–184.

Díaz A, Zikhali M, Turner AS, Isaac P, Laurie DA. 2012. Copy Number Variation Affecting the Photoperiod-B1 and Vernalization-A1 Genes Is Associated with Altered Flowering Time in Wheat (Triticum aestivum). PLoS ONE **7**, 1–11.

Eagles HA, Cane K, Kuchel H, Hollamby GJ, Vallance N, Eastwood RF, Gororo NN, Martin PJ. 2010. Photoperiod and vernalization gene effects in southern Australian wheat. Crop and Pasture Science **61**, 721–730.

Fischer RA. 1975. Yield Potential in a Dwarf Spring Wheat and the Effect of Shading. Crop Science **15**, 607–613.

Fischer RA. 1985. Number of kernels in wheat crops and the influence of solar radiation and temperature. The Journal of Agricultural Science **105**, 447–461.

Fischer RA. 2011. Wheat physiology: a review of recent developments. Crop and Pasture Science **62**, 95–114.

Foulkes J, Sylvester-Bradley R, Worland AJ, Snape JW. 2004. Effects of a photoperiod-response gene Ppd-D1 on yield potential and drought resistance in UK winter wheat. Euphytica, 63–73.

Garibaldi LA, Aristimuño FJ, Oddi FJ, Tiribelli F. 2017. Inferencia multimodelo en ciencias sociales y ambientales. Ecología Austral **27**, 348–363.

Gelman A, Carlin JB, Stern HS, Dunson DB, Vehtari A, Rubin DB. 2013. *Bayesian Data Analysis*. Boca Raton: Chapman and Hall/CRC.

González FG, Slafer GA, Miralles DJ. 2002. Vernalization and photoperiod responses in wheat pre flowering reproductive phases. Field Crops Research **74**, 183–195.

González FG, Slafer GA, Miralles DJ. 2005. Pre-anthesis development and number of fertile florets in wheat as affected by photoperiod sensitivity genes Ppd-D1 and Ppd-B1. Euphytica **146**, 253–269.

Griffiths FEW, Lyndon RF, Bennett MD. 1985. The Effects of Vernalization on the Growth of the Wheat Shoot Apex. Annals of Botany **56**, 501–511.

Halloran GH, Pennell AL. 1982. Duration and Rate of Development Phases in Wheat in Two Environments. Annals of Botany **49**, 115–121.

Hay R, Kirby EJM. 1991. Convergence and Synchrony - a Review of the Coordiation of Development in Wheat. Australian Journal of Agricultural Research **42**, 661–700.

He J, Le Gouis J, Stratonovitch P *et al.* 2012. Simulation of environmental and genotypic variations of final leaf number and anthesis date for wheat. European Journal of Agronomy **42**, 22–33.

Jamieson PD, Brooking IR, Semenov MA, Porter JR. 1998. Making sense of wheat development: A critique of methodology. Field Crops Research **55**, 117–127.

Jamieson PD, Brooking IR, Semenov MA, McMaster GS, White JW, Porter JR. 2007. Reconciling alternative models of phenological development in winter wheat. Field Crops Research **103**, 36–41.

Kamran A, Iqbal M, Spaner D. 2014. Flowering time in wheat (Triticum aestivum L.): A key factor for global adaptability. Euphytica **197**, 1–26.

Kass RE, Raftery AE. 1995. Bayes Factors. Journal of the American Statistical Association **90**, 773–795.

Lavine M, Schervish MJ. 1999. Bayes Factors: What They are and What They are Not. The American Statistician 53, 119–122.

Major DJ. 1980. Photoperiod response characteristics controlling flowering of nine crop species. Canadian Journal of plant Science **60**, 777–784.

McElreath RL. 2015. *Statistical Rethinking: A Bayesian Course with Examples in R and Stan*. CRC Press.

McIntosh RA, Yamazaki Y, Devos KM, Dubcovsky J, Rogers WJ, Appels R. 2003. Catalogue of Gene Symbols for Wheat. Tenth International Wheat Genetics Symposium.1–47.

Miralles DJ, Richards RA. 2000. Responses of Leaf and Tiller Emergence and Primordium Initiation in Wheat and Barley to Interchanged Photoperiods. Annals of Botany **85**, 655–663.

Miralles DJ, Slafer GA, Richards RA, Rawson HM. 2003. Quantitative developmental response to the length of exposure to long photoperiod in wheat and barley. The Journal of Agricultural Science **141**, 159–167.

Ochagavía H, Prieto P, Savin R, Griffiths S, Slafer G. 2017. Duration of developmental phases, and dynamics of leaf appearance and tillering, as affected by source and doses of photoperiod insensitivity alleles in wheat under field conditions. Field Crops Research **214**, 45–55.

Pérez-Gianmarco TI, Slafer GA, González FG. 2018. Wheat pre-anthesis development as affected by photoperiod sensitivity genes (Ppd-1) under contrasting photoperiods. Functional Plant Biology **45**, 645–657.

Piironen J, Vehtari A. 2017. Comparison of Bayesian predictive methods for model selection. Statistics and Computing **27**, 711–735.

R Core Team. 2018. *R: A Language and Environment for Statistical Computing*. Vienna, Austria: R Foundation for Statistical Computing.

Rosen J. 2016. A forest of hypotheses. Nature **536**, 239–241.

Royo C, Dreisigacker S, Alfaro C, Ammar K, Villegas D. 2015. Effect of Ppd-1 genes on durum wheat flowering time and grain filling duration in a wide range of latitudes. The Journal of Agricultural Science **154**, 612–631.

Scarth R, Law CN. 1984. The Control of the day-length Response in Wheat by the Group-2 Chromosomes. Zeitschrift fur Pflanzenzuchtung **92**, 140–150.

Scarth R, Kirby EJM, Law CN. 1985. Effects of the Photoperiod Genes Ppd1 and Ppd2 on Growth and Development of the Shoot Apex in Wheat. Annals of Botany **55**, 351–359.

Shaw LM, Turner AS, Laurie DA. 2012. The impact of photoperiod insensitive Ppd-1a mutations on the photoperiod pathway across the three genomes of hexaploid wheat (Triticum aestivum). The Plant Journal **71**, 71–84.

Slafer GA. 1996. Differences in phasic development rate amongst wheat cultivars independent of responses to photoperiod and vernalization. A viewpoint of the intrinsic earliness hypothesis. Journal of Agronomy and Crop Science **44**, 403–419.

Slafer GA, Rawson HM. 1994. Sensitivity of wheat phasic development to major environmental factors: A Re-examination of some assumptions made by physiologists and modellers. Australian Journal of Plant Physiology **21**, 393–426.

Slafer GA, Halloran GM, Connor DJ. 1994. Development Rate in Wheat as Affected by Duration and Rate of Change of Photoperiod. Annals of Botany **73**, 671–677.

Slafer GA, Rawson HM. 1996. Responses to photoperiod change with phenophase and temperature during wheat development. Field Crops Research **46**, 1–13.

Slafer GA, Rawson HM. 1997. Phyllochron in Wheat as Affected by Photoperiod Under Two Temperature Regimes. Australian Journal of Plant Physiology **24**, 151–158.

Slafer GA, Abeledo LG, Miralles DJ, Gonzalez FG, Whitechurch E. 2001. Photoperiod sensitivity during stem elongation as an avenue to raise potential yield in wheat. Euphytica **119**, 191–197.

Snape JW, Butterworth K, Whitechurch E, Worland AJ. 2001. Waiting for fine times: Genetics of flowering time in wheat. Euphytica **119**, 185–190.

Stelmakh AF. 1997. Genetic systems regulating flowering response in wheat. In: Braun HJ, In: Altay F, In: Kronstad WE, In: Beniwal SPS, In: McNab A, eds. Wheat: Prospects for Global Improvement: Proceedings of the 5th International Wheat Conference, 1014 June, 1996, Ankara, Turkey. Dordrecht: Springer Netherlands, 491–501.

Vehtari A, Gelman A, Gabry J. 2017. Practical Bayesian model evaluation using leave-one-out cross-validation and WAIC. Statistics and Computing **27**, 1413–1432.

Vince Prue D. 1975. *Photoperiodism in plants*. McGraw-Hill: London & New York. [Review in Nature 258 (1975) p. 462 by H. Smith.] University textbook. Textbk, Photoperiodism, General_article (PMBD, 185610419).

Wallach D, Makowski D, Jones JW, Brun F (Eds.). 2014. *Working with dynamic crop models: methods, tools and examples for agriculture and environment*. Amsterdam: Elsevier/Academic Press.

White JW, Herndl M, Hunt LA, Payne TS, Hoogenboom G. 2008. Simulation-Based Analysis of Effects of Vrn and Ppd Loci on Flowering in Wheat. Crop Science **48**, 678–687.

Whitechurch EM, Slafer GA. 2002. Contrasting Ppd alleles in wheat: Effects on sensitivity to photoperiod in different phases. Field Crops Research **73**, 95–105.

Whitechurch EM, Slafer GA, Miralles DJ. 2007. Variability in the Duration of Stem Elongation in Wheat Genotypes and Sensitivity to Photoperiod and Vernalization. Journal of Agronomy and Crop Science **193**, 131–137.

Wilhelm EP, Turner AS, Laurie DA. 2009. Photoperiod insensitive Ppd-A1a mutations in tetraploid wheat (Triticum durum Desf.). Theoretical and Applied Genetics **118**, 285–294.

Worland AJ. 1996. The influence of flowering time genes on environmental adaptability in European wheats. Euphytica **89**, 49–57.

Yin X, van der Linden CG, Struik PC. 2018. Bringing genetics and biochemistry to crop modelling, and vice versa. European Journal of Agronomy **100**, 132–140.

Zadoks JC, Chang TT, Konzak CF. 1974. A decimal code for the growth stages of cereals. **14**, 415–421.

Zheng B, Biddulph B, Li D, Kuchel H, Chapman S. 2013. Quantification of the effects of VRN1 and Ppd-D1 to predict spring wheat (Triticum aestivum) heading time across diverse environments. Journal of Experimental Botany **64**, 3747–3761.

FIGURE LEGENDS

Figure 1: Photoperiod (dashed lines) and daily mean temperature (circles and solid lines) progression through the growing season for each year in which experiments were held. Numbers by dashed lines indicate the number of hours by which natural photoperiod including civil twilight was extended to obtain such photoperiod values. Daily mean temperatures are indicated by closed circles, for sowings within usual sowing dates, and by open circles for the late-season experiment in 2018. Full arrows indicate time of emergence and thin arrows are placed at the date the last anthesis was registered for each experiment. The earlier pair of arrows in 2018 correspond to usual sowing dates and the later pair stand for the late-season experiment.

Figure 2: Schematic representation of photoperiod extension treatments. The width of each flow represents the number of seasons that a treatment was performed at and its colour is set according to initial photoperiod extension treatments, from emergence to onset of stem elongation (EM-OSE). Flow ends in coincidence with the photoperiod treatment to which it was transferred at OSE and stayed at until anthesis (AN).

Figure 3: Graphical representation of the effect of *Ppd-1* genes on the response to photoperiod of three hypothetical genotypes varying in their *Ppd-1* allelic combination (blue, red, and green response curves), as would be described by models E, I, and H, from left to right.

Figure 4: Thermal time from emergence to anthesis as related to mean photoperiod and *Ppd-1* allelic combination, as described by model E (see Eq. 1). Each line shows the mean value of the sample from posterior distribution for each genotype (fit), the shade extends to the upper and lower limits of the 90% credible interval. Data used to fit the model is shown using different symbols and colours for each of the five genotypes. Five genotypes representative of the variability in model E parameters of the total 14 allelic combinations fitted are shown. For data and fits on all 14 allelic combinations, please refer to Supplementary Figure 1.

Figure 5: Photoperiod sensitivity as related to number of *Ppd-1a* alleles carried by near-isogenic lines (NILs).

Figure 6: Duration of particular developmental phases to mean current or previous photoperiod and *Ppd-1* allelic combination as described by model T (see Eq. 2).

Developmental phases shown are EM-OSE, from emergence to onset of stem elongation, OSE-FL, from onset of stem elongation to flag leaf appearance, and FL-AN, from flag leaf appearance to anthesis. Each line shows the mean value of the sample from posterior distribution for each genotype (fit), the shade extends to the upper and lower limits of the 90% credible interval. Data used to fit the model is shown using different symbols and colours for each of the five genotypes. Five genotypes representative of the variability in model T parameters of the total 14 allelic combinations fitted are shown. For data and fits on all 14 allelic combinations, please refer to Supplementary Figure 2.

Figure 7: Relationship between fitted and observed values for selected models E (from the first set) and model T (form the second set) and root mean square error (RMSE) of the relationship. Data from different years are represented using points of different shapes and colours.

Table 1: Genotype of each near-isogenic line (NIL) in A, B, and D genomes. *Ppd-1a* alleles are associated with photoperiod-insensitive phenotypes and *Ppd-1b* ones with the sensitive wild type.

	Allelic combination			
NIL Name	*Ppd-A1*	*Ppd-B1*	*Ppd-D1*	*Ppd-1a* donor
Paragon	*b*	*b*	*b*	
PR2B	*b*	*a*	*b*	Recital
PCS2B	*b*	*a*	*b*	Chinese Spring
PS642B	*b*	*a*	*b*	Sonora 64
PGS1002A	*a*	*b*	*b*	GS-100
PS642D	*b*	*b*	*a*	Sonora 64
PO2D	*b*	*b*	*a*	Opata
PCS2B+S642D	*b*	*a*	*a*	
PS642B+S642D	*b*	*a*	*a*	
PGS1002A+CS2B	*a*	*a*	*a*	
PGS1002A+S642B	*a*	*a*	*a*	
PGS1002A+S642D	*a*	*a*	*a*	
PGS1002A+CS2B+S642D	*a*	*a*	*a*	
PGS1002A+S642B+S642D	*a*	*a*	*a*	

Table 2: Description of models proposed for the response of accumulated thermal time to anthesis to photoperiod. In bold, the model chosen (described in detail in Eq. 1).

		Considers *Ppd-1* effects on model parameters?		
Model	Type of response	Constant (α)	Sensitivity (β)	Threshold photoperiod (γ)
A	linear	YES	NO	N/A
B	linear	YES	YES	N/A
C	bi-linear	NO	NO	NO
D	bi-linear	YES	YES	NO
E	**bi-linear**	**NO**	**YES**	**NO**
F	bi-linear	YES	NO	YES
G	bi-linear	NO	YES	YES
H	bi-linear	YES	NO	NO
I	bi-linear	NO	NO	YES
J	bi-linear	YES	YES	YES

Table 3: Description of proposed models of response to photoperiod considering each pre-anthesis phase. In bold, the model chosen (described in detail in Eq. 2).

	Phase sensitive to photoperiod?			Parameter affected by *Ppd-1* genes?						
Model	EM-OSE	OSE-FL	FL-AN	constant $\alpha^{\text{EM-OSE}}$	sensitivity $\beta^{\text{EM-OSE}}$	threshold $\gamma^{\text{EM-OSE}}$	constant $\alpha^{\text{OSE-FL}}$	sensitivity (c) $\beta^{\text{OSE-FL}}$	sensitivity (p) $\delta^{\text{EM-OSE}}$	constant $\alpha^{\text{FL-AN}}$
A	YES	NO	NO	NO	YES	NO	N/A	N/A	N/A	N/A
B	YES	YES (c)	NO	NO	YES	NO	NO	NO	N/A	N/A
C	YES	YES (c)	NO	NO	YES*	NO	YES*	NO - YES	N/A	YES	N/A
D	YES	YES (c)	NO	NO	YES*	NO	YES*	NO - YES	N/A	YES	YES
E	YES	YES (c)	YES	NO	YES	NO	NO	NO	N/A		NO
F	YES	YES (c)	YES	NO	NO	YES	NO	NO	N/A		NO
G	YES	YES (c)	YES	YES	NO	NO	NO	NO	N/A		NO
H	YES	YES (c)	YES	NO	YES	YES	NO	NO	N/A		NO
I	YES	YES (c)	YES	YES	NO	YES	NO	NO	N/A		NO
J	YES	YES (c)	YES	YES	YES	YES	NO	NO	N/A		NO
K	YES	YES (c)	YES	NO	YES	NO	YES	NO	N/A		NO
L	YES	YES (c)	YES	NO	YES*	NO	YES*	NO	N/A		NO
M	YES	YES (c)	YES	NO	YES*	NO	YES*	NO	N/A		YES

	Phase sensitive to photoperiod?			Parameter affected by *Ppd-1* genes?						
Model	EM-OSE	OSE-FL	FL-AN	constant $\alpha^{EM\text{-}OSE}$	sensitivity $\beta^{EM\text{-}OSE}$	threshold $\gamma^{EM\text{-}OSE}$	constant $\alpha^{OSE\text{-}FL}$	sensitivity (c) $\beta^{OSE\text{-}FL}$	sensitivity (p) $\delta^{EM\text{-}OSE}$	constant $\alpha^{FL\text{-}AN}$
N^{+}	YES	YES (c)	YES	NO	YES*	NO	YES*	NO	N/A	YES
O	YES	YES (c)	YES	NO	NO	YES*	YES*	NO	N/A	YES
P	YES	YES (c)	YES	YES*	NO	NO	YES*	NO	N/A	YES
Q	YES	YES (c)	YES	NO	YES*	YES*	YES*	NO	N/A	YES
R	YES	YES (c)	YES	YES*	NO	YES*	YES*	NO	N/A	YES
S	YES	YES (c)	YES	YES*	YES*	YES*	YES*	NO	N/A	YES
T	YES	**YES (c, p)**	YES	NO	YES*	NO	YES*	NO	YES*	YES
U	YES	YES (c, p)	YES	YES	YES*	YES	YES*	NO	YES*	YES
V	YES	YES (c, p)	YES	NO	YES*	NO	YES*	YES	YES	YES

+: Model N differs from model M and others in that it is the only one not considering residuals' correlations.

**: Correlation between these parameters across pre-anthesis phases is considered in the model.*

(c) and (p) are used to differentiate between response to either current (c) or previous (p) photoperiod.

Table 4: Performance of each model from the first set, ranked by their difference in expected predictive accuracy according to cross-validation (Δ EPA-CV) relative to the best performing model and standard error of that difference. R^2 and root mean square error (RMSE) for observed and fitted values of anthesis are also provided.

Model	Δ EPA-CV (± s.e.)	R^2	RMSE
G	0.00 ± 0.0	0.71	106.7
E	**-0.01 ± 0.34**	**0.71**	**106.7**
D	-0.26 ± 0.27	0.71	106.7
J	-0.32 ± 0.28	0.71	106.7
B	-77.36 ± 19.43	0.67	113.1
F	-138.40 ± 18.63	0.64	119.0
I	-138.40 ± 18.68	0.64	119.0
H	-157.10 ± 21.16	0.63	120.7
A	-195.70 ± 23.07	0.60	124.4
C	-453.90 ± 44.5	0.40	152.5

Table 5: Values of the parameters of models E and model T for each NIL (or *Ppd-1* combination of alleles). The mean and 90% Credible Interval are provided as obtained by sampling from the posterior distributions of each model.

	Model E	Model T			
NIL Name	β_j	$\beta_j^{\text{EM-OSE}}$	$\alpha_j^{\text{OSE-FL}}$	$\delta_j^{\text{OSE-FL}}$	$\alpha_j^{\text{FL-AN}}$
genotype	$^oC\ d\ h^{-1}$	$^oC\ d\ h^{-1}$	$^oC\ d$	$^oC\ d\ h^{-1}$	$^oC\ d$
Paragon	-162	-138	936	-25	415
Ppd-A1b, Ppd-B1b, Ppd-D1b	(-153, -171)	(-126, -149)	(877, 995)	(-22, -29)	(393, 437)
PCS2B	-88	-67	669	-12	395
Ppd-A1b, Ppd-B1a, Ppd-D1b	(-83, -93)	(-61, -73)	(632, 708)	(-10, -14)	(375, 437)
PR2B	-85	-64	658	-12	404
Ppd-A1b, Ppd-B1a, Ppd-D1b	(-79, -92)	(-57, -71)	(612, 707)	(-9, -15)	(384, 426)
PS642B	-73	-56	594	-9	398
Ppd-A1b, Ppd-B1a, Ppd-D1b	(-68, -78)	(-50, -62)	(553, 635)	(-6, -11)	(378, 418)
PGS1002A	-68	-49	570	-8	396
Ppd-A1a, Ppd-B1b, Ppd-D1b	(-63, -73)	(-43, -55)	(528, 610)	(-5, -10)	(376, 416)
PS642D	-63	-47	568	-8	388
Ppd-A1b, Ppd-B1b, Ppd-D1a	(-59, -69)	(-42, -52)	(530, 608)	(-5, -10)	(367, 409)
PO2D	-56	-42	534	-6	386
Ppd-A1b, Ppd-B1b, Ppd-D1a	(-51, -61)	(-37, -47)	(494, 574)	(-3, -8)	(369, 409)
PGS1002A+CS2B	-58	-36	543	-5	387
Ppd-A1a, Ppd-B1a, Ppd-D1b	(-53, -63)	(-31, -41)	(501, 582)	(-2, -7)	(368, 407)
PS642B+S642D	-56	-38	551	-7	386
Ppd-A1b, Ppd-B1a, Ppd-D1a	(-51, -61)	(-33, -44)	(512, 591)	(-4, -9)	(367, 406)
PGS1002A+S642B	-55	-37	553	-6	387
Ppd-A1a, Ppd-B1a, Ppd-D1b	(-50, -60)	(-32, -42)	(514, 593)	(-4, -9)	(367, 407)
PGS1002A+S642D	-50	-28	543	-6	383
Ppd-A1a, Ppd-B1b, Ppd-D1a	(-45, -55)	(-23, -33)	(501, 588)	(-3, -8)	(363, 403)
PCS2B+S642D	-49	-31	537	-5	383
Ppd-A1b, Ppd-B1a, Ppd-D1a	(-44, -54)	(-26, -36)	(498, 581)	(-3, -8)	(363, 403)
PGS1002A+S642B+S642D	-48	-34	498	-3	382
Ppd-A1a, Ppd-B1a, Ppd-D1a	(-43, -53)	(-30, -40)	(451, 538)	(0, -6)	(363, 403)
PGS1002A+CS2B+S642D	-44	-27	513	-4	382
Ppd-A1a, Ppd-B1a, Ppd-D1a	(-39, -49)	(-22, -32)	(473, 553)	(-2, -7)	(362, 402)

β_j: *photoperiod sensitivity from EM to AN*
$\beta_j^{EM\text{-}OSE}$: *photoperiod sensitivity from EM to OSE*
$\alpha_j^{OSE\text{-}FL}$: *constant for the OSE-FL duration*
$\delta_j^{OSE\text{-}FL}$: *sensitivity to previous photoperiod during OSE to FL*
$\alpha_j^{FL\text{-}AN}$: *constant for the FL-AN duration*

Table 6: Performance of each model from the second set, ranked by their difference in

Model	Δ EPA-CV (± s.e.)	*K*	R^2			RMSE
			EM-OSE	OSE-FL	FL-AN	

expected predictive accuracy according to cross-validation (Δ EPA-CV) relative to the simplest best performing model and standard error of that difference. *K* resumes Bayes factors results of comparing model T against the other best performing models*. R^2 and root mean square error (RMSE) for observed and fitted values of anthesis are also shown.

U	0.0 ± 0.0	6.7×10^{1}	0.78	0.38	0.16	100.8
T	**-11.5 ± 4.5**	*****	**0.77**	**0.39**	**0.15**	**101.1**
V	-11.6 ± 4.5	4.7×10^{6}	0.77	0.39	0.15	101.1
S	-112.0 ± 17.6	1.5×10^{46}	0.79	0.25	0.16	101.5
M	-117.0 ± 17.9	2.9×10^{43}	0.79	0.26	0.15	101.2
Q	-119.3 ± 17.8	4.6×10^{46}	0.79	0.26	0.15	101.3
L	-135.5 ± 19.5	-	0.79	0.26	0.13	102.0
K	-135.7 ± 19.5	-	0.79	0.26	0.13	102.0
N	-172.0 ± 22.1	-	0.77	0.25	0.16	102.6
D	-216.1 ± 22.1	-	0.795	0.27	0.02	103.0
J	-218.6 ± 27.9	-	0.80	0.14	0.13	106.4
C	-223.8 ± 21.5	-	0.79	0.27	0.00	103.4
O	-228.9 ± 22.1	-	0.75	0.25	0.16	108.1
R	-228.9 ± 22.2	-	0.75	0.25	0.16	108.1
E	-234.2 ± 28.4	-	0.79	0.14	0.13	108.4
H	-234.2 ± 22.7	-	0.79	0.14	0.13	106.7
B	-323.0 ± 30.1	-	0.79	0.14	0.00	109.9
F	-334.2 ± 30.3	-	0.76	0.14	0.13	113.1
I	-334.3 ± 30.3	-	0.76	0.14	0.13	113.1
P	-403.9 ± 33.8	-	0.67	0.25	0.16	120.1
A	-416.1 ± 29.7	-	0.79	0.00	0.00	120.0
G	-508.6 ± 40.1	-	0.67	0.14	0.13	125.7

**Values bigger than 10^{1} show strong evidence in favour of model T (Kass and Raftery, 1995).*

Table 7: Final leaf number (mean and standard deviation) under five different photoperiod extension treatments during the EM-OSE phase, as averaged across seasons.

Genotype	**Photoperiod extension treatment during the EM-OSE phase**									
	+0		**+2**		**+4**		**+6**		**+8**	
	Mean	S.D.	Mean	S.D.	Mean	S.D.	Mean	S.D.	Mean	S.D.
Paragon	11.8	1.20	9.8	0.42	7.8	1.26	7.5	1.32	6.0	0.00
PR2B	9.9	0.82	8.1	0.92	6.9	0.88	6.5	0.76	6.5	0.71
PCS2B	9.6	1.20	8.1	0.85	7.1	1.02	7.1	1.10	6.0	0.00
PS642B	9.3	0.99	8.0	0.65	7.1	0.42	7.2	1.00	6.0	
PGS1002A	9.1	1.04	7.9	1.39	7.1	0.79	7.1	0.93	6.0	0.00
PS642D	9.3	1.06	8.3	0.84	7.0	0.80	7.2	0.98	6.5	0.71
PO2D	8.9	1.11	7.4	0.48	6.7	0.87	6.8	0.83	6.0	
PCS2B+S642D	8.2	1.04	7.7	0.67	6.7	1.07	6.7	0.78	6.5	0.71
PS642B+S642D	8.7	1.18	7.8	1.04	6.9	0.98	6.8	0.86	6.0	
PGS1002A+CS2B	8.4	0.92	7.7	0.99	7.5	0.65	7.1	0.78	7.0	0.00
PGS1002A+S642B	8.5	0.87	7.7	1.32	6.8	0.76	6.8	0.88	6.0	
PGS1002A+S642D	8.2	0.96	7.4	1.07	6.7	0.84	6.7	0.83	6.0	0.00
PGS1002A+CS2B+S642D	7.9	1.11	7.4	0.56	6.9	0.82	6.7	0.77	6.0	0.00
PGS1002A+S642B+S642D	8.0	1.05	6.9	1.40	6.6	0.89	6.7	0.93	6.5	0.71

For genotype descriptions see Table 1.

Fig. 1

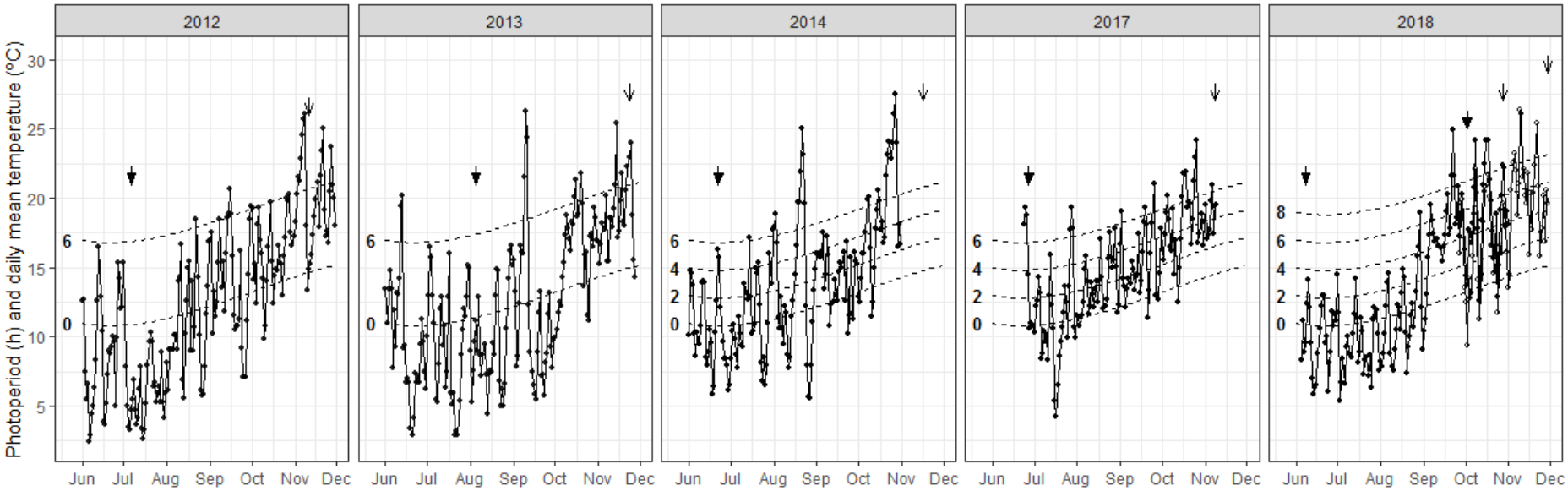

Fig. 2

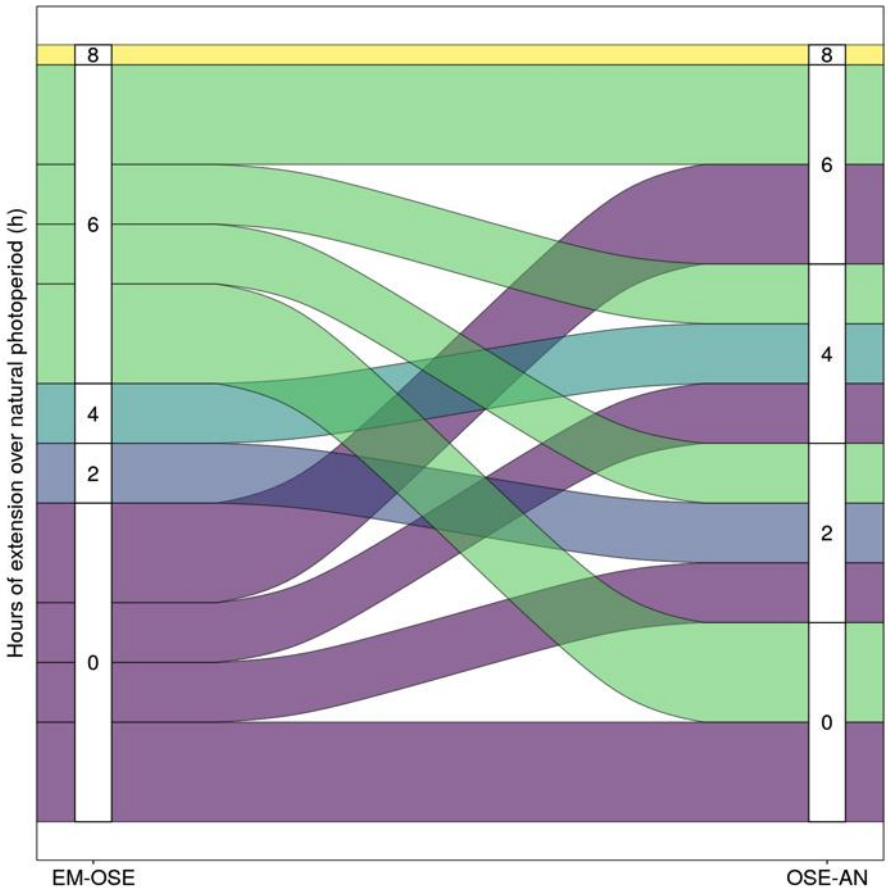

Fig. 3

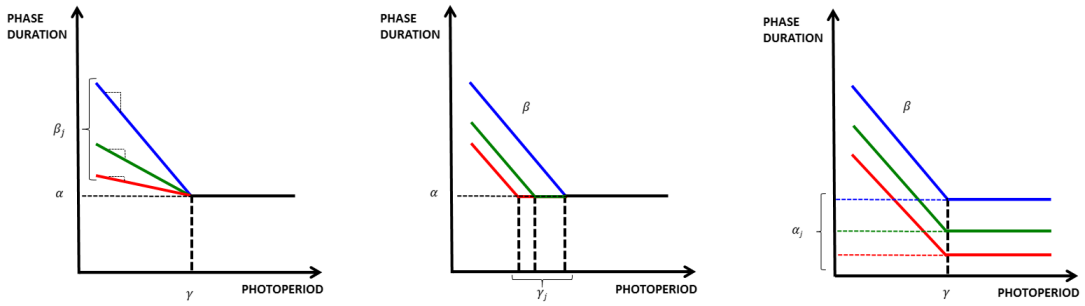

Fig. 4

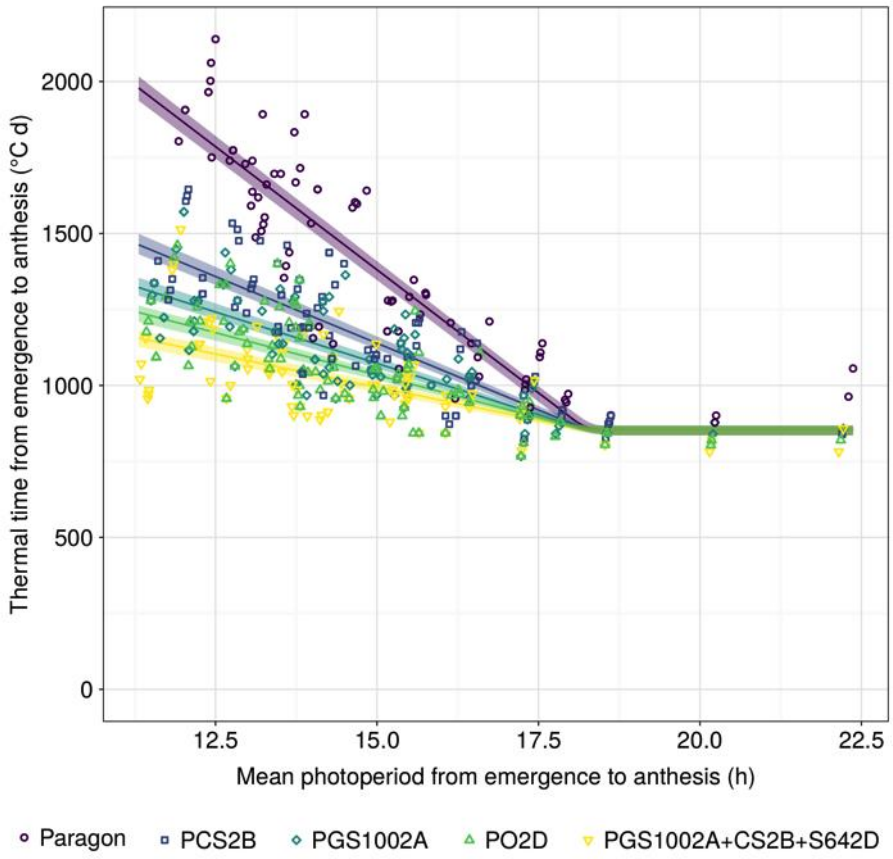

Fig. 5

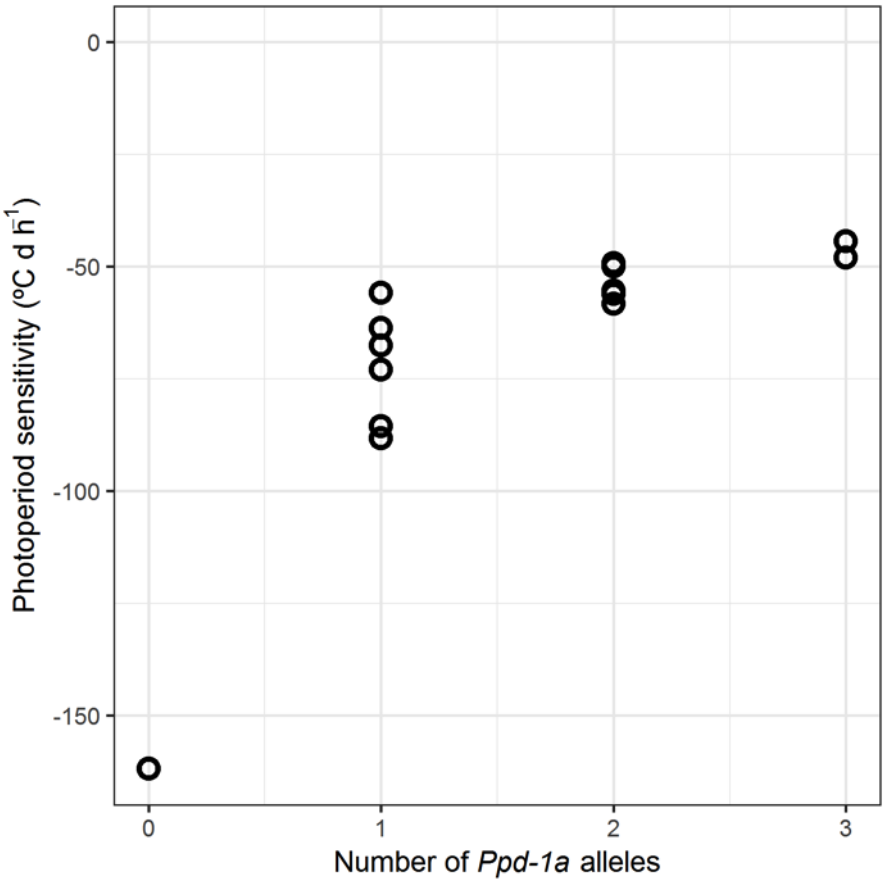

Fig. 6

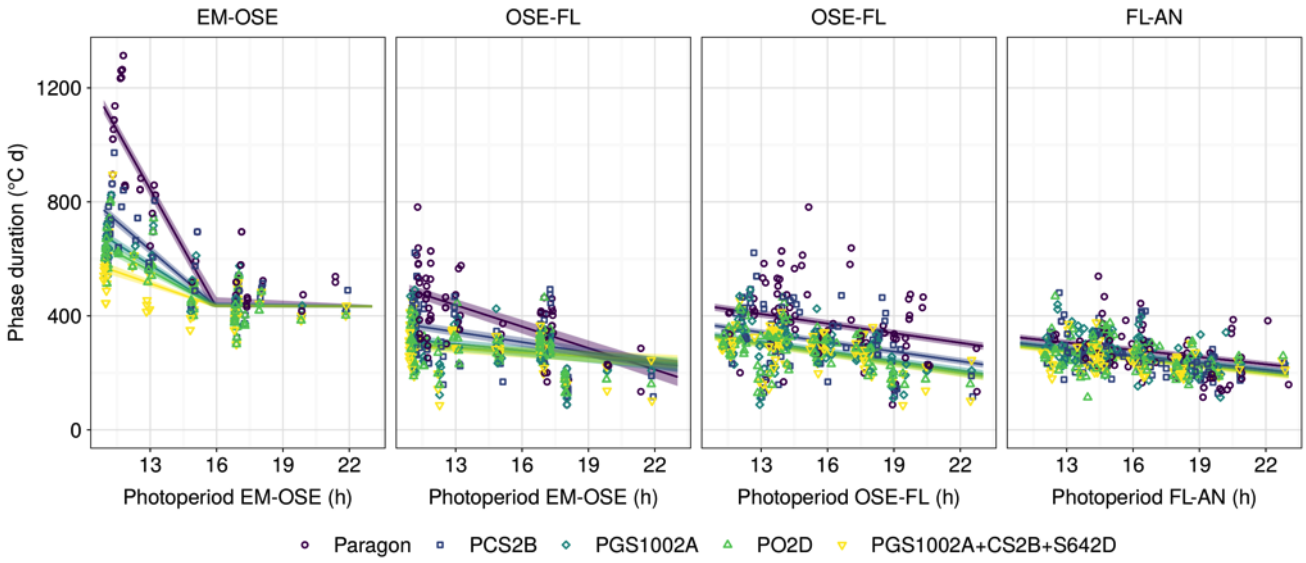

Fig. 7